

EFFECTS OF THERMAL STRATIFICATION ON FLOW AND HEAT TRANSFER DUE TO A STRETCHING CYLINDER WITH UNIFORM SUCTION/INJECTION

Ali J. Chamkha*, M.M. Abd El-Aziz °, Sameh E. Ahmed**

*Manufacturing Engineering Department, The Public Authority for Applied Education and Training,

Shuweikh 70654, Kuwait, E-mail: achamkha@yahoo.com

°Department of Mathematics, South Valley University, Qena, Egypt

**Department of Mathematics, South Valley University, Qena, Egypt, E-mail: sameh_sci_math@yahoo.com

ABSTRACT

In this paper, a numerical solution of flow and heat transfer outside a stretching permeable cylinder with thermal stratification and suction/injection effects is investigated. The governing system of partial differential equations is converted to ordinary differential equations by using suitable similarity transformations which are then solved using a numerical technique. A parametric study is performed to study the effects of the governing parameters, namely the suction/injection parameter, thermal stratification parameter, Prandtl number and Reynolds number on the velocity profiles, pressure distribution and temperature profiles as well as the skin-friction coefficient and the Nusselt number. The velocity, pressure and temperature results are shown graphically whereas the values of the skin-friction coefficient and the Nusselt number are presented in tables. It is found that water is a better cooling agent compared to air provided that there is no strong injection.

Keywords: Heat transfer, suction/injection, stretching cylinder, thermal stratification.

1. INTRODUCTION

In many mixed flows of practical importance in nature as well as in many engineering devices, the environment is thermally stratified. The discharge of hot fluid into enclosed regions often results in a stable thermal stratification with a lighter fluid overlying a denser fluid. The thermal stratification effects of heat transfer over a stretching surface is of interest in polymer extrusion processes where the object, after passing through a die, enters the fluid for cooling below a certain temperature. The rate at which such objects are cooled has an important bearing on the properties of the final product. In the process of cooling the fluids, the momentum boundary layer for linear stretching of sheet was first studied by Crane [1].

In addition, the study of heat transfer a round cylinders have received considerable attention from the researchers. Ahmed et al. [2] presented a numerical study of heat transfer in a conical annular cylinder fixed with saturated porous medium. The problem of laminar natural convection boundary layer flow on an isothermal vertical thin cylinder embedded in a thermally stratified high porosity medium is studied by Takhar et al. [3]. They found that, the skin friction coefficient vanishes for certain values of the stratification parameter or the curvature parameter. Nguyen et al. [4] investigated heat transfer from a rotating circular cylinder immersed in a spatially uniform, time-dependent convective environment. Hassanien et al. [5] developed a numerical procedure, based on Chebyshev polynomials for the steady micropolar fluid in

the vicinity of an axisymmetric stagnation point flow on a cylinder. Saeid [6] used the thermally non-equilibrium model to study the free convection from a horizontal cylinder immersed in porous media. The effect of temperature-dependent viscosity on the natural convection heat transfer from a horizontal isothermal cylinder of elliptic cross section was studied by Cheng [7]. Ishak et al. [8] discussed the effect of uniform suction/blowing on flow and heat transfer due to a stretching cylinder. The study of steady flow in a viscous and incompressible fluid outside of a stretching hollow cylinder in an ambient fluid at rest was done by Wang [9].

The main objective of this paper is to study thermal stratification and uniform suction/blowing effects on flow and heat transfer due to a stretching cylinder. Similarity transformations are used to transform the partial differential equations to ordinary differential equations which then are solved numerically. The present study represents an extension of the work of Wang [9] by including thermal stratification and suction/injection effects.

2. PROBLEM FORMULATION

Consider steady laminar, incompressible flow caused by a stretching circular tube of radius a in the axial direction in a fluid at rest as shown in Fig. 1. The z -axis is measured along the axis of the tube and the r -axis is measured in the radial direction. It is assumed that the temperature variation of the tube is taken into account and is also given by the power-law

temperature, $T_w - T_\infty = Az^n$ where A and n are constants. The viscous dissipation is neglected as it is assumed to be small. Under these assumptions, the governing equations are.

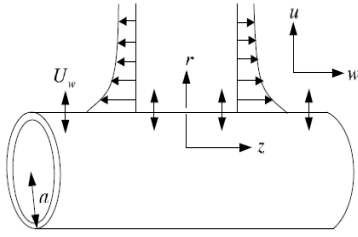


Fig. 1. Physical model and coordinate system.

$$\frac{\partial w}{\partial z} + \frac{\partial u}{\partial r} + \frac{u}{r} = 0, \tag{1}$$

$$w \frac{\partial w}{\partial z} + u \frac{\partial w}{\partial r} = \nu \left(\frac{\partial^2 w}{\partial r^2} + \frac{1}{r} \frac{\partial w}{\partial r} \right), \tag{2}$$

$$w \frac{\partial u}{\partial z} + u \frac{\partial u}{\partial r} = -\frac{1}{\rho} \frac{\partial p}{\partial r} + \nu \left(\frac{\partial^2 u}{\partial r^2} + \frac{1}{r} \frac{\partial u}{\partial r} - \frac{u}{r^2} \right), \tag{3}$$

$$w \frac{\partial T}{\partial z} + u \frac{\partial T}{\partial r} = \alpha \left(\frac{\partial^2 T}{\partial r^2} + \frac{1}{r} \frac{\partial T}{\partial r} \right), \tag{4}$$

subject to the boundary conditions

$$\begin{aligned} r = a: \quad & u = U_w, \quad w = w_w, \\ & T = T_w(z) = T_\infty(z) + Az^n \\ r \rightarrow \infty: \quad & w \rightarrow 0, \quad T = T_\infty(z) = (1-n)T_0 + nT_w(z) \\ & = T_0 + \frac{n}{1-n} Az^n \end{aligned} \tag{5}$$

where $U_w = -ca\gamma$, $w_w = 2cz$, c is a positive constant and γ is a constant such that $\gamma > 0$ and $\gamma < 0$ corresponding to mass suction and mass injection, respectively. In addition, n is a constant which is the thermal stratification parameter such that $0 \leq n < 1$. The constant n is defined as the thermal stratification parameter and is equal to $m_1/(1+m_1)$ of Nakayama and Koyama [10] where m_1 is a constant. T_0 is a constant reference temperature say, $T_\infty(0)$. The suffices W and ∞ denote surface and ambient conditions.

Following Wang [9] we take the similarity transformation:

$$\begin{aligned} \eta = (r/a)^2, \quad u = -ca \left[F(\eta)/\sqrt{\eta} \right], \quad w = 2czF'(\eta) \\ , \quad \theta(\eta) = (T - T_\infty)/(T_w - T_\infty), \end{aligned} \tag{6}$$

where a prime denotes ordinary differentiation with respect to η . Substituting Eqs. (6) into Eqs. (2) and (4), we will get the following ordinary differential equations:

$$\eta F''' + F'' + \text{Re} [FF'' - F'^2] = 0, \tag{7}$$

$$\eta \theta'' + \theta' [1 + \text{PrRe}F] - n \text{PrRe}F' \left(\theta + \frac{n}{1-n} \right) = 0, \tag{8}$$

where $\text{Re} = ca^2/2\nu$ is the Reynolds number, $\text{Pr} = \mu C_p / K$ is the Prandtl number where K is thermal conductivity.

$$\begin{aligned} \text{The dimensionless boundary conditions (5) become} \\ F(1) = \gamma, \quad F'(1) = 1, \quad \theta(1) = 1, \quad F' \rightarrow 0, \\ \theta \rightarrow 0 \text{ as } \eta \rightarrow \infty. \end{aligned} \tag{9}$$

The pressure p can now be determined from Eq. (3) in the form

$$\frac{p - p_\infty}{\rho c \nu} = -\frac{\text{Re}}{\eta} F^2(\eta) - 2F'(\eta), \tag{10}$$

Physical quantities of interest are the skin-friction coefficient C_f and the Nusselt number Nu which are defined as

$$C_f = \frac{\tau_w}{\rho w_w^2 / 2}, \quad \text{Nu} = \frac{aq_w}{K(T_w - T_\infty)}. \tag{11}$$

Further, τ_w and q_w are the shear stress and the heat transfer from the surface of the tube, respectively, and they are given by

$$\tau_w = \left[\mu \frac{\partial w}{\partial r} \right]_{r=a}, \quad q_w = -K \left(\frac{\partial T}{\partial r} \right)_{r=a}. \tag{12}$$

Substituting Eqs. (6) and (12) into Eq. (11) yields

$$\left(\frac{\text{Re}z}{a} \right) C_f = F''(1), \quad \text{Nu} = -2\theta'(1), \tag{13}$$

3. NUMERICAL METHOD

The numerical procedure used here solves the two-point boundary value problems for a system of N ordinary differential equations in the range (x, x_1) . The system is written as and the derivatives

$$\frac{dy_i}{dx} = f_i(x, y_1, y_2, \dots, y_N) \quad i = 1, 2, \dots, N$$

are evaluated by a procedure that evaluates the derivatives of y_1, y_2, \dots, y_N at general point x . Initially, N boundary values of the variable y_i must be specified, some of which will be specified at x and some at x_1 . The remaining N boundary values are guessed and the procedure corrects them by a form of Newtonian iteration. Starting from the known and guessed values of y_i at x , the procedure integrates the equations forward to a matching point R , using Merson's method. Similarly, starting from x_1 it integrates backwards to R . The difference between the forward and backward values of y_i at R should be zero for a true solution. The procedure uses a generalized Newton method to reduce these differences to zero, by calculating corrections to the estimated boundary values. This process is repeated iteratively until convergence is obtained to as specified accuracy. The tests for convergence and the perturbation of the boundary conditions are carried out in a mixed form, e.g., if the error estimate for y_i is ERROR_i , we test whether $\text{ABS}(\text{ERROR}_i) < \text{ERROR}_i \times (1 + \text{ABS}(y_i))$. This numerical method employed is found to be accurate and suitable and gives results very close to the results obtained by Wang [9]. Table 1 shows a comparison between the present results and the results obtained by Wang [9]. It can be seen that a very good agreement between the results exists.

4. RESULTS AND DISCUSSION

In order to get a clear insight of the physical problem, numerical results are displayed with the help of tables and graphical illustrations. Representative numerical results are

presented in Figs. 2-10 and Tables 1-4 to illustrate the influence of several non-dimensional parameters, namely Reynolds number Re , Prandtl number Pr , thermal stratification parameter n and suction/injection parameter γ . For the reference case for the results $Pr = 0.7, -0.5 \leq \gamma \leq 0.5, n = 0.2$, and $Re = 3.0$.

Table 1. Comparison of $F''(1)$ with Wang [9] for impermeable surface case

Re	Wang [9]	Present work
0.5	-0.88220	-0.88700
1.0	-1.17776	-1.17953
2.0	-1.59390	-1.59444
5.0	-2.41745	-2.41798

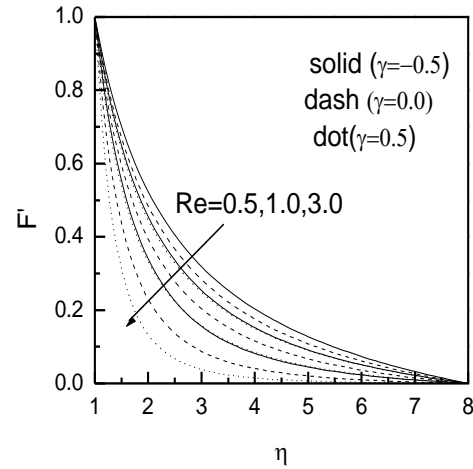


Fig. 3. Velocity profiles for various values of Re

4.1 Velocity profiles

It is clear from the momentum equation (7) that the thermal stratification parameter n and the Prandtl number Pr have no effect on the velocity profile as it is uncoupled from the energy equation (8). Fig. 2 shows the velocity profiles for various values of the suction/injection parameter γ . It is observed from this figure and is true in all cases, that the velocity vanishes at some large distance from the surface of the tube and it decreases with increasing values of γ . In addition, Fig. 3 displays the effect of Reynolds number Re on the velocity distributions. The Reynolds number represents the relative significance of inertia effects compared to the viscous effects. Thus, as Re increases, the velocity profiles in the boundary layer decrease. It is also observed from Figs. 2 and 3 that increasing the suction/injection parameter γ and the Reynolds number Re results in decreases in the hydrodynamic boundary-layer thickness.

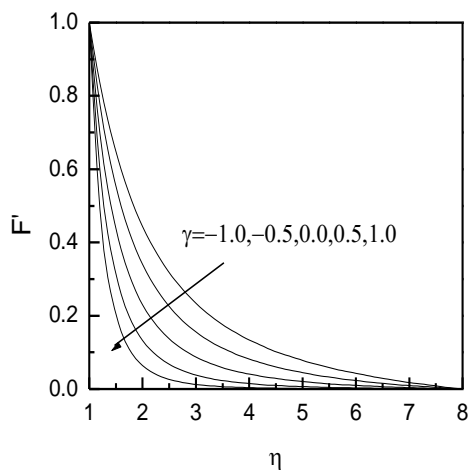


Fig. 2. Velocity profiles for various values of γ

4.2 Pressure distributions

After the velocity distribution $F(\eta)$ is obtained, the pressure distribution P in terms of $(P - P_\infty)/\rho cv$ can be found from Eq. (10). The numerical results for the pressure distribution are shown in Figs. 4 and 5 for various values of the suction/injection parameter γ and the Reynolds number Re , respectively. All curves show that $P \rightarrow P_\infty$ far away from the surface ($\eta \rightarrow \infty$). It is observed from Fig. 4 that increasing the suction or injection parameter γ produces reductions in the pressure distribution whereas Fig. 5 shows that increasing the Reynolds number results in higher pressure distribution.

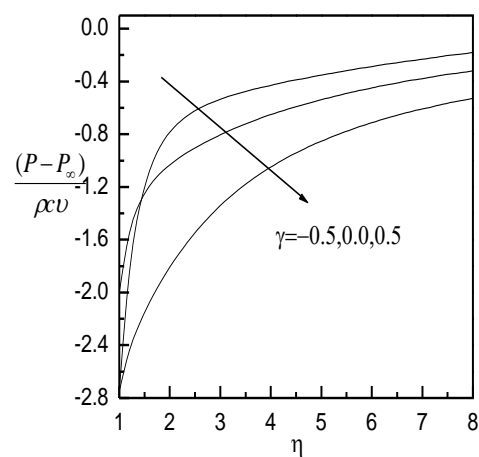


Fig. 4. Pressure distribution $(P - P_\infty)/\rho cv$ obtained from Eq. (10) for various values of γ

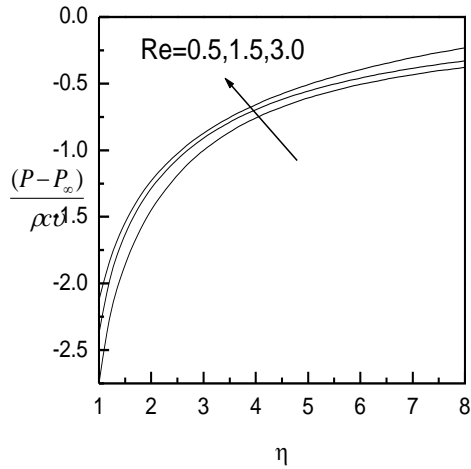


Fig. 5. Pressure distribution $(P - P_\infty)/\rho U l^{0.5}$ obtained from Eq. (10) for various values of Re and $\gamma = 0.5$

4.3 The similarity profiles $F(\eta)$

The similarity profiles $F(\eta)$ for various values of Re and γ are shown in Fig. 6. It is clear from the boundary condition (9) that $F(\eta)$ starting from the value of γ and increases until takes the final predicted value $F(\infty)$ far away from the cylinder surface (see Table 2). Therefore, as γ increases, the similarity profiles $F(\eta)$ increase. Moreover, it is predicted that increasing the value of Re leads to decreases in the similarity profiles $F(\eta)$.

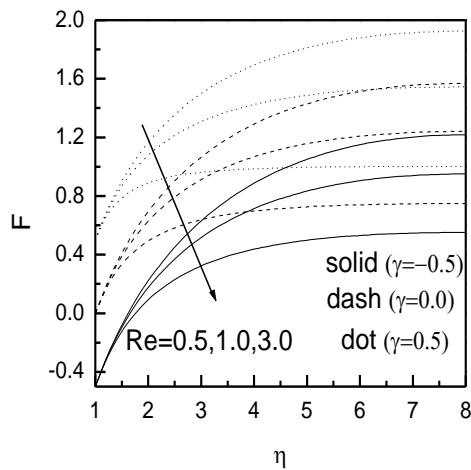


Fig. 6. Similarity profiles $F(\eta)$ for various values of Re and γ

4.4 Temperature distributions

The physical model of the problem (Fig. 1) neglects the effect of gravitation force or thermal buoyancy force in favor of the stretching effect. This means that the flow problem is uncoupled from the thermal one. Representative dimensionless temperature profiles θ are presented for various values of the thermal stratification parameter n , suction/injection parameter γ and the Prandtl number Pr in Figs. 7-10, respectively. These figures clearly show that the fluid temperature decreases by increasing either of n , γ or Pr . In all cases, the temperature vanishes at some large distance from the surface and therefore, gives some information on the thermal boundary layer thickness. It is seen from these figures that the thermal boundary layer thickness decreases significantly by increasing either of n , γ or Pr and that this effect is compounded if they are increased together.

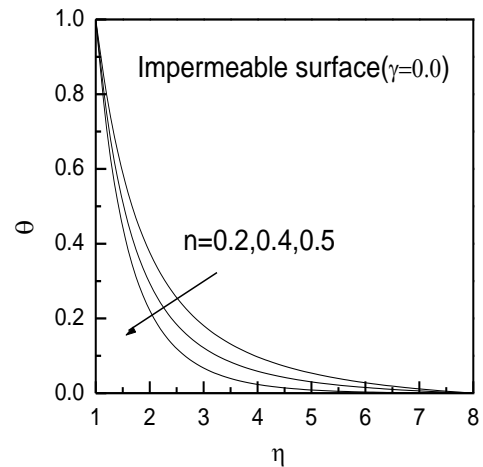


Fig. 7. Temperature distributions for various values of n

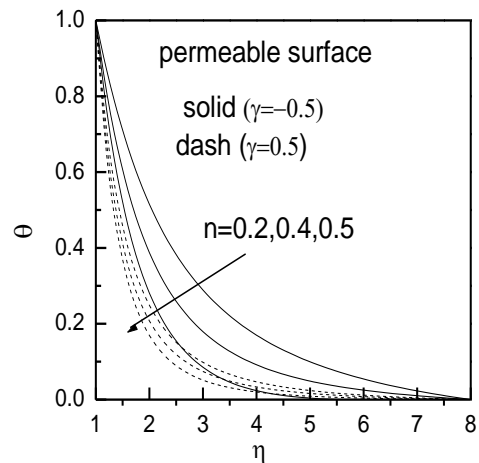


Fig. 8. Temperature distributions for various values of n and γ

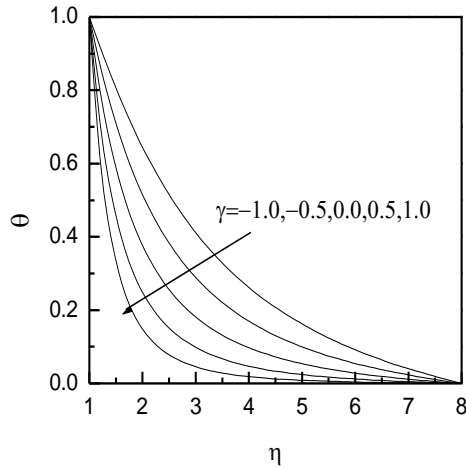


Fig. 9. Temperature distributions for various values of γ

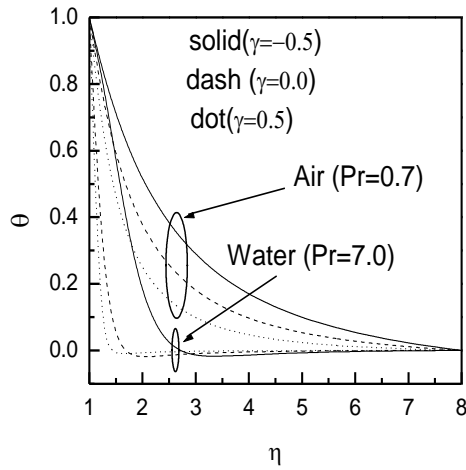


Fig. 10. Temperature distributions for various values of Pr

4.5 Skin-friction coefficient

Table 2 presents some values of $F''(1)$ (which represents the skin-friction coefficient) for various parametric conditions [see Eq. (13)]. It is observed that all these values are negative. Physically, a negative sign of $F''(1)$ implies that the stretching tube or cylinder exerts a dragging force on the fluid and a positive sign implies the opposite. In addition, Table 2 shows that increasing the value of the transpiration parameter γ results in an increase in the absolute values of the skin-friction coefficient $F''(1)$. Moreover, as the Reynolds number Re increases, the absolute value of $F''(1)$ or the skin-friction coefficient increases. Table 3 shows values of $F(\infty)$ for various values of Re and γ . It is seen that $F(\infty)$ decreases with Re and increases with γ .

Table 2. Values of the skin-friction coefficient $F''(1)$ for various values of Re and γ

Re	Impermeable Surface	Permeable Surface	
	$\gamma = 0.0$	$\gamma = -0.5$	$\gamma = 0.5$
0.5	-0.88700	-0.78948	-1.01312
1.0	-1.17953	-0.96339	-1.44159
2.0	-1.59444	-1.18123	-2.14717
3.0	-1.91551	-1.31714	-2.77573

Table 3. Values of $F(\infty)$ for various values of Re and γ

Re	Impermeable Surface	Permeable Surface	
	$\gamma = 0.0$	$\gamma = -0.5$	$\gamma = 0.5$
0.5	1.56891	1.21753	1.92519
1.0	1.24035	0.95014	1.54435
2.0	0.91735	0.6878	1.18168
3.0	0.74888	0.55109	1.00301

4.6 Nusselt number

Tables 4-6 illustrate the influence of the Reynolds number Re , Prandtl number Pr , suction/injection parameter γ and the thermal stratification parameter n on the rate of heat transfer or Nusselt number. It is predicted that increasing the values of either of the Reynolds number Re , suction/injection parameter γ or the thermal stratification parameter n produces increases in the values of the Nusselt number. Also, for the case of impermeable surface and the case suction condition, increasing the value of the Prandtl number Pr causes the Nusselt number to increase but, for the injection case, as the Prandtl number Pr increases from 0.2 to 7.0, the Nusselt number decreases from 0.79049 to 0.63593 (see Tables 4-6)

Table 4. Values of Nusselt number $-\theta'(1)$ for various values of Re and γ

Re	Impermeable Surface	Permeable Surface	
	$\gamma = 0.0$	$\gamma = -0.5$	$\gamma = 0.5$
0.5	0.65717	0.57347	0.74912
1.0	0.78582	0.62263	0.97759
2.0	0.98731	0.67385	1.39534
3.0	1.15053	0.69646	1.79046

Table 5. Values of Nusselt number $-\theta'(1)$ for various values of Pr and γ

Pr	Impermeable Surface	Permeable Surface	
	$\gamma = 0.0$	$\gamma = -0.5$	$\gamma = 0.5$
0.7	1.15053	0.69646	1.79046
2.0	2.10655	0.79049	4.24349
7.0	4.23743	0.63593	12.53812

Table 6. Values of Nusselt number $-\theta'(1)$ for various values of n and γ

n	Impermeable Surface	Permeable Surface	
	$\gamma = 0.0$	$\gamma = -0.5$	$\gamma = 0.5$
0.2	1.15053	0.69646	1.79046
0.4	1.49384	1.05998	2.07105
0.6	2.22261	1.79925	2.68882
0.8	4.47949	4.03338	4.64507

4. CONCLUSION

This paper focused on steady two-dimensional flow of an incompressible fluid due to a stretching permeable tube with uniform suction/injection and thermal stratification effects. The governing equations are transformed into self-similar equations and are solved numerically by an integration technique. A parametric study of the physical parameters such as the thermal stratification parameter, Prandtl number, Reynolds number and the suction/injection parameter is conducted to illustrate the influence of these parameters on the flow and heat transfer characteristics. From this investigation, we can draw the following conclusions:

1. The fluid velocity and the hydrodynamic boundary-layer thickness decreased as either of the suction/injection parameter or the Reynolds number increased.
2. The pressure distribution reduced as the suction/blowing parameter was increased.
3. The fluid temperature and the thermal boundary-layer thickness decreased significantly by increasing either of the suction/injection parameter, thermal stratification parameter or the Prandtl number. The skin-friction coefficient increased with increasing values of either the Reynolds number or the

suction/injection parameter while it remained constant with increasing values of the thermal stratification parameter and Prandtl number.

4. The rate of heat transfer increased by increasing either of the suction/injection parameter, thermal stratification parameter or the Prandtl number.

Nomenclature

A	constant
a	radius of cylinder
c	positive constant
C_f	skin friction coefficient
C_p	specific heat of the fluid
F	similarity variable
K	thermal conductivity
n	thermal stratification parameter
Nu	Nusselt number
P	pressure
Pr	Prandtl number
Re	Reynolds number
T	dimensional temperature
u, w	dimensional velocity components
r, z	dimensional coordinates

Greek symbols

α	thermal diffusivity
η	dimensionless coordinate
μ	dynamic viscosity
ν	kinematic viscosity
ρ	density
γ	suction/injection parameter
θ	dimensionless temperature

Subscript

W	Conditions at wall
∞	Conditions far away from wall

6. REFERENCES

- [1] L. J. Crane, Z. Angew, Second-order fluid flow past a stretching sheet with heat transfer, Math. Phys. Vol. 21, pp. 641–647, 1970.
- [2] N. J. S. Ahmed, I. A. Badruddin, Z. A. Zainal, H. M. T. Khaleed, J. Kanesan, Heat transfer in a conical cylinder with porous medium, Int. J. Heat Mass Transfer, vol 52, pp. 3070–3078, 2009.
- [3] H. S. Takhar, A. J. Chamkha, G. Nath, Natural convection on a vertical cylinder embedded in a thermally stratified high-porosity medium, Int. J. Therm. Sci. vol, 41, pp. 83–93, 2002.
- [4] H. D. Nguyen, S. Paik, R. W. Douglass, Unsteady mixed convection about a rotating circular cylinder with small fluctuations in the free-stream velocity, vol. 39, pp. 511–525, 1996.
- [5] A. Hassanien, H. M. El-hawary, A. A. Salama, chebyshev solution of axisymmetric stagnation flow on a cylinder, Energy Convers. Mgmt. vol. 37, pp. 67–76, 1996.

- [6] N. H. Saeid, Analysis of free convection about a horizontal cylinder in a porous media using a thermal non-equilibrium model, *Int. Commu. Heat MassTransfer* vol. 33, pp. 158–165, 2006.
- [7] C-Y. Cheng, The effect of temperature- dependent viscosity on the natural convection heat transfer from a horizontal isothermal cylinder of elliptic cross section, *Int. Commu. Heat MassTransfer* vol. 33, pp. 1021–1028, 2006.
- [8] A. Ishak, R. Nazar, I. Pop, Uniform suction/blowing effect on flow and heat transfer due to a stretching cylinder, *Appl. Math. Modell.* Vol. 32, pp. 2059–2066, 2008.
- [9] C. Y. Wang, Fluid flow due to a stretching cylinder, *Phys. Fluids* vol. 31, 466–468, 1988.
- [10] A. Nakayama, H. Koyama, Similarity solutions for buoyancy induced flows over a non isothermal curved surface in a thermally stratified porous medium, *Appl. Sci. Res.* 46 (1989) 309–322.

THE MATERIAL WITHIN THIS PAPER, AT THE AUTHOR'S (AUTHORS') RESPONSIBILITY, HAS NOT BEEN PUBLISHED ELSEWHERE IN THIS SUBSTANTIAL FORM NOR SUBMITTED ELSEWHERE FOR PUBLICATION. NO COPYRIGHTED MATERIAL NOR ANY MATERIAL DAMAGING THIRD PARTIES INTERESTS HAS BEEN USED IN THIS PAPER, AT THE AUTHOR'S (AUTHORS') RESPONSIBILITY, WITHOUT HAVING OBTAINED A WRITTEN PERMISSION.